





**AUTHORS:**

Edward J. Odes<sup>1</sup>   
Alexander H. Parkinson<sup>2</sup>   
Patrick S. Randolph-Quinney<sup>1,2,3</sup>   
Bernhard Zipfel<sup>2,4</sup>  
Kudakwashe Jakata<sup>2</sup>  
Heather Bonney<sup>5</sup>  
Lee R. Berger<sup>2</sup> 

**AFFILIATIONS:**

<sup>1</sup>School of Anatomical Sciences, University of the Witwatersrand, Johannesburg, South Africa

<sup>2</sup>Evolutionary Studies Institute, University of the Witwatersrand, Johannesburg, South Africa

<sup>3</sup>School of Forensic and Applied Sciences, University of Central Lancashire, Preston, Lancashire, United Kingdom

<sup>4</sup>School of Geosciences, University of the Witwatersrand, Johannesburg, South Africa

<sup>5</sup>Department of Earth Sciences, Natural History Museum, London, United Kingdom

**CORRESPONDENCE TO:**

Edward J. Odes

**EMAIL:**

eddieodes@gmail.com

**DATES:**

**Received:** 17 May 2016

**Revised:** 07 Sep. 2016

**Accepted:** 08 Sep. 2016

**KEYWORDS:**

Sterkfontein; micro computed tomography; spinal degenerative joint disease; palaeopathology; taphonomy

**HOW TO CITE:**

Odes EJ, Parkinson AH, Randolph-Quinney PS, Zipfel B, Jakata K, Bonney H, et al. Osteopathology and insect traces in the *Australopithecus africanus* skeleton StW 431. *S Afr J Sci.* 2017;113(1/2), Art. #2016-0143, 7 pages. <http://dx.doi.org/10.17159/sajs.2017/20160143>

**ARTICLE INCLUDES:**

- ✓ Supplementary material
- × Data set

**FUNDING:**

DST/NRF Centre of Excellence in Palaeosciences; National Research Foundation (South Africa); University of the Witwatersrand

© 2017. The Author(s).  
Published under a Creative Commons Attribution Licence.

# Osteopathology and insect traces in the *Australopithecus africanus* skeleton StW 431

We present the first application of high-resolution micro computed tomography in an analysis of both the internal and external morphology of the lumbar region of StW 431 – a hominin skeleton recovered from Member 4 infill of the Sterkfontein Caves (South Africa) in 1987. The lumbar vertebrae of the individual present a number of proliferative and erosive bony processes, which were investigated in this study. Investigations suggest a complex history of taphonomic alteration to pre-existing spinal degenerative joint disease (SDJD) as well as post-mortem modification by an unknown insect. This study is in agreement with previous pathological diagnoses of SDJD which affected StW 431 and is the first time insect traces on this hominin are described. The results of this analysis attest to the complex series of post-mortem processes affecting the Sterkfontein site and its fossil assemblages.

**Significance:**

- First application of high-resolution micro computed tomography of the lumbar region of StW 431, a partial skeleton of *Australopithecus africanus*, attests to pre-existing degenerative joint disease and identifies post-mortem modification by an unknown insect.
- The co-occurrence of degenerative pathology and insect modification may not be unique to StW 431. A combination of traditional morphoscopic analysis and non-invasive high-resolution tomography is recommended.

## Introduction

The StW 431 hominin skeleton was discovered by excavation teams from the University of the Witwatersrand during February and March 1987,<sup>1</sup> at the karstic cave site of Sterkfontein, Cradle of Humankind, South Africa. This site has yielded the largest sample of the taxon *Australopithecus africanus*, fossil members of the genus *Homo* and archaeological evidence of Oldowan and more recent lithic technologies.<sup>2-7</sup>

The StW 431 specimen comprises a partial skeleton of *Australopithecus africanus*, consisting of 48 fragments reconstructed into 18 partial elements.<sup>1</sup> The skeletal remains (Figure 1) consist of portions of the right scapula and clavicle, right humerus, radius and ulna, a right rib, five thoracic vertebrae, five lumbar vertebrae, the first three sacral segments and os coxae, and part of the right acetabulum. The individual is skeletally adult (based on sacral vertebral fusion) and has been previously assigned as male on the basis of a number of morphological characteristics. These characteristics include overall robusticity and muscular markers, the proportions between the body of the first sacral segment and the sacral base, and a relatively large estimated body mass (41.1–42.5 kg) based on reduced major axis regression consistent with the male range of body size for *A. africanus*.<sup>1</sup> The postcranial remains were associated to a single individual, based partly on position, refit, similar colour and physical condition, state of preservation and morphology.<sup>1</sup>

Stratigraphic understanding of the site at the time of excavation attributed the remains to Bed B of Member 4 within the Sterkfontein Formation.<sup>1</sup> While the exact chronological age of this stratigraphic bed is unknown, age estimates range between 1.5 Ma and 2.8 Ma for the member as a whole.<sup>2-7</sup> It is widely acknowledged that accurate dating of South African cave sites has been historically problematical.<sup>8</sup> Age ranges of between 2.4 mya and 2.8 mya of Sterkfontein Member 4 have been established by faunal analysis and archaeology<sup>9-12</sup>, where absolute dating methods have proved problematic<sup>13</sup>. Electron spin resonance methods have also been used to date South African Plio-Pleistocene sites, and dates between 1.6 mya and 2.87 mya for Member 4 Sterkfontein have been suggested, with an average electron spin resonance estimated age of  $2.1 \pm 0.5$  Ma.<sup>14</sup> Using U-Pb dating methods, a new absolute age range of between  $2.65 \pm 0.30$  Ma and  $2.01 \pm 0.05$  Ma has been assigned to fossiliferous deposits of Sterkfontein Member 4.<sup>15</sup> Electron spin resonance, isotopic and palaeomagnetic studies carried out on speleothem and siltstone material from Member 4 Sterkfontein Cave suggests the date of the deposits and *A. africanus* fossils at between 2.58 Ma and 2.16 Ma. Thus largely based on arguments of parsimony, provenance and morphology, most researchers studying the skeleton have accepted a taxonomic assignment to *A. africanus*.<sup>16,17</sup>

StW 431 is additionally important as the skeleton has been cited with regard to ongoing debate concerning the presence of skeletal pathology in the specimen; researchers have previously identified two conditions – brucellosis and spondylosis deformans – affecting this specimen.<sup>18,19</sup> Staps<sup>18</sup> diagnosed spondylosis deformans with osteophytic formation, and osteoarthritis of the facet joints from L4 to S1. In contradistinction, D’Anastasio and colleagues<sup>19</sup> diagnosed a case of possible brucellosis. In this paper, we attempt to resolve this debate and clarify the nature of ante- versus post-mortem processes affecting the specimen.



Scale = 50 mm

**Figure 1:** StW 431 – a partial skeleton of *Australopithecus africanus* discovered at Sterkfontein Caves in 1937. Stw 431 represented only the third partial skeleton attributed at the time to *A. africanus*, and represents the only probable male skeleton attributed to this taxon to date.

## Materials and methods

The fourth and fifth lumbar vertebrae of StW 431 were studied macro- and microscopically to record surface morphology. Internal bone structure was imaged using micro computed tomography (micro-CT). Comparative skeletal material – including healthy modern human and pathological vertebrae from the Bone Teaching Collection and Raymond A. Dart Collection of Human Skeletons housed in the School of Anatomical Sciences at the University of the Witwatersrand – was also imaged. Comparative material with known and purported brucellar pathology from radiographical and palaeopathological literature was also studied (see Supplementary table 1 for a list of all comparative materials used in this study).

Gross surface morphology of the vertebral specimens was studied microscopically at magnifications of 7–25 times under reflected light using an Olympus SZX 16 multifocus microscope fitted with a digital camera. Micrographic imaging of the anterior and lateral bodies, antero-superior margins and endplates of the two lumbar vertebrae was carried out by applying Analysis 5.0, which includes a Z-stacking function. This function operates as an automated smoothing process whereby multiple sub-images are transformed into a single high-quality, high-resolution image with greater depth of field than a single micrograph.

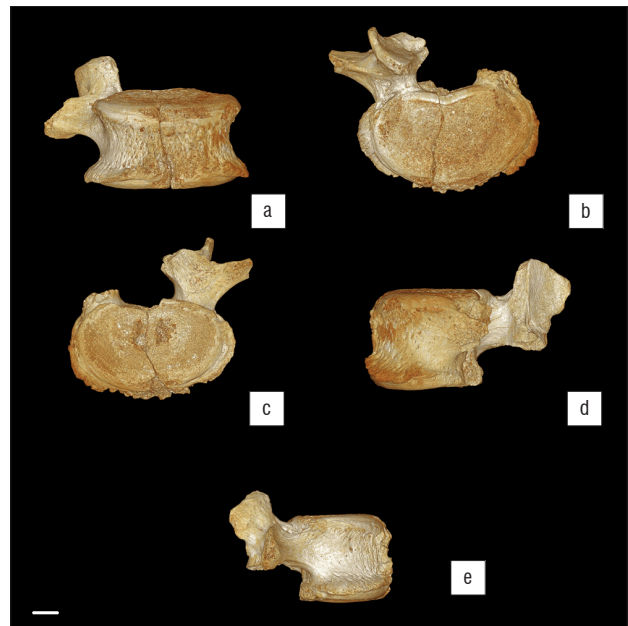
In order to investigate internal (as well as external) morphology, imaging of the StW 431 vertebral specimens was carried out using micro-CT undertaken with a Nikon Metrology XTH 225/320 LC dual source industrial CT system housed in the Evolutionary Studies Institute of the University of the Witwatersrand. Both specimens were scanned using

a potential difference of 85 kV and a current of 75  $\mu$ A at a resolution of 33  $\mu$ m; a TIFF format image stack was generated in VG Studio Max following volume reconstruction. Further reconstruction was undertaken using Avizo Amira 5.4 to generate both two-dimensional orthoslice and three-dimensional surface rendered views based on the volume data; multiplanar mode was used to allow the recovery of homologous orthoslices (superior, inferior, coronal and sagittal) through both specimens for comparative purposes.

## Results

### Macroscopic analysis

The fourth lumbar vertebra (L4) is largely complete (Figure 2) and presents as the bulk of the vertebral centrum, the right pedicle, with right superior articular and transverse processes. Some degree of post-mortem damage has occurred, resulting in the loss of the left pedicle, lamina and superior, inferior and transverse processes. The remaining superior and transverse processes display some degree of post-mortem damage, with apices of both processes truncated, leading to exposure of internal trabeculae. The vertebral body further displays a fracture which runs slightly antero-laterally from the margin of the vertebral foramen to the anterior border of the body, just to the right of the midline. This fracture has led to the loss of a wedge of cortical bone at the antero-inferior margin of the centrum, with loss of cortex and exposure of underlying trabecular bone either side of the plane of the fracture. This erosion is contiguous with a zone of cortical erosion affecting the anterior surface of the body, with greatest removal of cortex on the left side of the body. Additionally, there is a small area of post-mortem erosion at the antero-superior rim of the centrum, on either side of the fracture, which has shaved off part of the labrum of the body over approximately 5–7 mm of the margin.



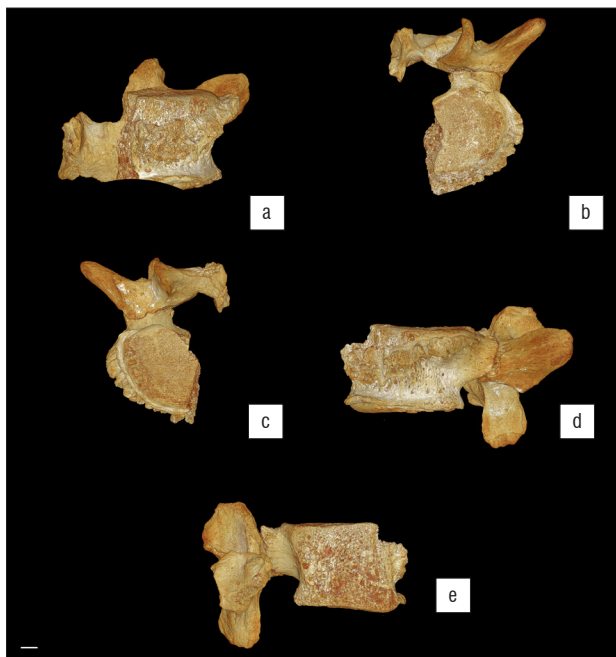
Scale = 10 mm

**Figure 2:** Three-dimensional volume rendered micro-CT views of the L4 vertebra of StW 431: (a) anterior, (b) superior, (c) inferior, (d) left lateral and (e) right lateral.

Slight osteophytic lipping occurs around the antero-superior region of L4, which creates a rolled appearance to the margin of the labrum, which is further disturbed by the erosion of this surface (Figure 2a). Extensive osteophytosis is expressed around the circumference of the inferior border of the vertebral body, present as a crenulated skirt of bone running from the anterior roots of the pedicles (the pedicle on the left, remaining as a short stump of the original process) around the margin of the body (Figure 2b,c). This skirt projects anteriorly a maximum of 5 mm beyond the inferior margin, and is most pronounced at the lateral

borders of the body. The superior endplate exhibits a generalised pattern of mild porosity. The surface of the inferior endplate exhibits more extensive erosion, with two major areas of cortical loss on either side of the midline of the vertebra – these are approximately 4 mm by 5 mm in diameter, the left of which is transected by the fracture which runs through the body.

The fifth lumbar vertebra (Figure 3) is less complete than L4 (Figure 2), displaying extensive post-mortem fracturing and damage. L5 presents as the left half of the vertebral body, with the pedicle, superior and inferior articular processes, and transverse process largely intact. The left lamina is present, together with a small portion of right lamina still attached, thus preserving a significant portion of the spinous process. In keeping with L4, L5 exhibits extensive osteophytic deposition, but both superior and inferior endplate margins, and the anterior surface of the body in the midline, which forms a series of cranio-caudally orientated buttresses, are more pronounced on the lateral side of the body. The osteophytic lipping extends from the left pedicle antero-laterally and continues anteriorly until it reaches the most anterior point of the vertebral body before it is interrupted by the fracture, which slices through the approximate midpoint of the vertebral body. The anterior projection of the superior osteophytic formation is interrupted by a large zone of removal of osseous tissue, which presents as a scooped, hollowed-out region that has removed both the osteophytic rim and a portion of the anterior body (Figure 3): this zone of removal has previously been described elsewhere as a region of osteolysis, possibly related to the presence of infectious disease.<sup>19</sup>



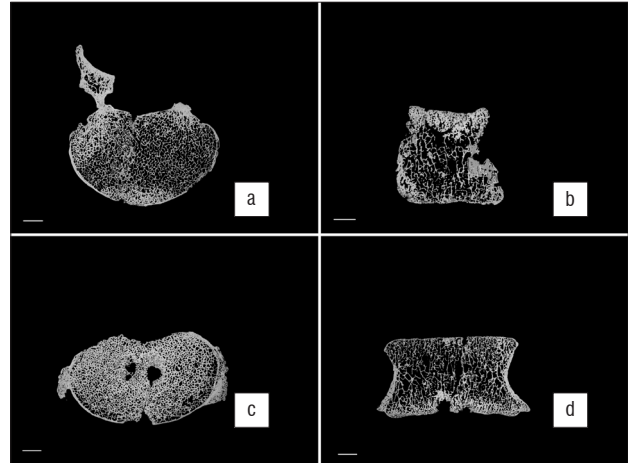
Scale = 10 mm

**Figure 3:** Three-dimensional volume rendered micro-CT views of the L5 vertebra of StW 431: (a) anterior, (b) superior, (c) inferior, (d) left lateral and (e) right lateral. Note the osteophytic formation on the superior and inferior endplate margins, as well as the anterior surface of the body in midline.

### Microscopic analysis

Micro-tomographic imaging of the internal morphology of L4 indicates areas of both bone deposition and removal. The superior body displays very slight osteophytic lipping around the antero-superior margin, which overall presents a slightly rolled appearance in cross section. This is clearly seen in Figure 4a,b, with a slight degree of remodelling and an increase in trabecular thickness and concomitant reduction in trabecular spacing in the antero-superior margin of the centrum. The greatest expression of osteophytosis occurs in the inferior body, where the original cortical bone making up the surface of the body can be seen

(Figure 4c). Secondly extensive areas of new bone formation of varying densities (from open woven to sclerotic) can be seen in transverse and coronal sections (Figure 4c,d). In addition to the marginal osteophytes, the two zones of endplate erosion are clearly evidenced. These appear as punched out cavities within the inferior body, where struts of individual trabeculae are truncated (and subsequently infilled with breccia in areas) with no evidence of sclerosis or reactive bone formation around the cavity margins (Figure 4c).

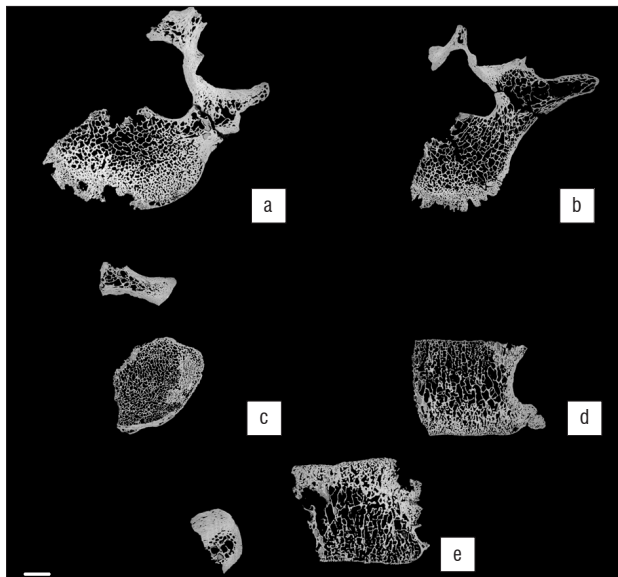


Scale = 10 mm

**Figure 4:** Micro-CT orthoslice views of the L4 vertebra of StW 431: (a) transverse superior, (b) sagittal midline, (c) transverse inferior and (d) anterior. Note the bilateral osteophytic formation and two zones of erosion evident on the inferior endplate surface of the L4 in (c). There is no evidence of sclerosis or new bone formation around the margins of the cavities (c). Also note areas of new bone formation ranging from open woven (c) to sclerotic (d).

In keeping with gross morphological assessment, micro-tomographic imaging of the internal morphology of L5 indicates extensive areas of both bone deposition and removal, with pronounced osteophytosis affecting the superior, anterior and inferior margins of the vertebral body. Figure 5a shows a transverse cross section through the superior region of the endplate (just inferior to the labrum), which demonstrates the extensive projection of osteophytes at the antero-superior margin. Unlike those affecting L4, these osteophytes express as direct remodelling of the cortical bone, appearing as both a thickened sclerotic margin and as crenulated buttresses of porous bone devoid of internal trabeculae; such a pattern is further reflected in the mid-transverse region of the body (Figure 5b). The inferior endplate, on the other hand, only presents osteophytosis as a thin ordered sclerotic rim extending around the inferior circumference, without buttressing (Figure 5c).

The pattern of erosion affecting L4 was identified by us (AHP) as being of potential post-mortem origin, and specifically surface modification caused by insects. In order to clarify this modification, potential insect damage was further imaged at magnifications between 7x and 115x using an Olympus SZX 16 multifocus microscope fitted with a digital camera. Terminologies used to describe the morphology of traces observed is based on a recent summary of general morphologies of bioerosional traces in bone.<sup>20</sup> Length and width measurements were taken using Stream Essentials<sup>®</sup> image processing software linked to the Olympus SZX multifocus microscope. Depth measurements were obtained using digital callipers. Two comparative collections of insect damage to bone were utilised in this study: these experimental collections comprise bones exposed to the following agents under control conditions; a southern African termite (*Trinervitermes trinervoides*)<sup>21</sup> and a dermestid beetle (*Dermestes maculatus*)<sup>22</sup>. Furthermore, insect damage was compared to available data gleaned from the literature.<sup>21-24</sup>



Scale = 10 mm

**Figure 5:** Micro-CT orthoslice views of the L5 vertebra of StW 431: (a,b) transverse to the midline (close to surface), (c) transverse to inferior, (d) coronal midline, (e) sagittal superior to bottom. Note new bone formation on the anterior wall (e) and major osteophytic formation at the antero-superior margin indicating remodelling of the cortex, revealing a sclerotic margin, and as crenulated buttresses of porous bone devoid of internal trabeculae (a,b). There is no evidence of sclerosis or reactive bone formation around the cavity margins (a). The inferior endplate (c) exhibits an osteophytic formation as a thin ordered sclerotic rim around inferior circumference with no presence of buttressing. Notice the channel interpreted as invertebrate damage in (e).

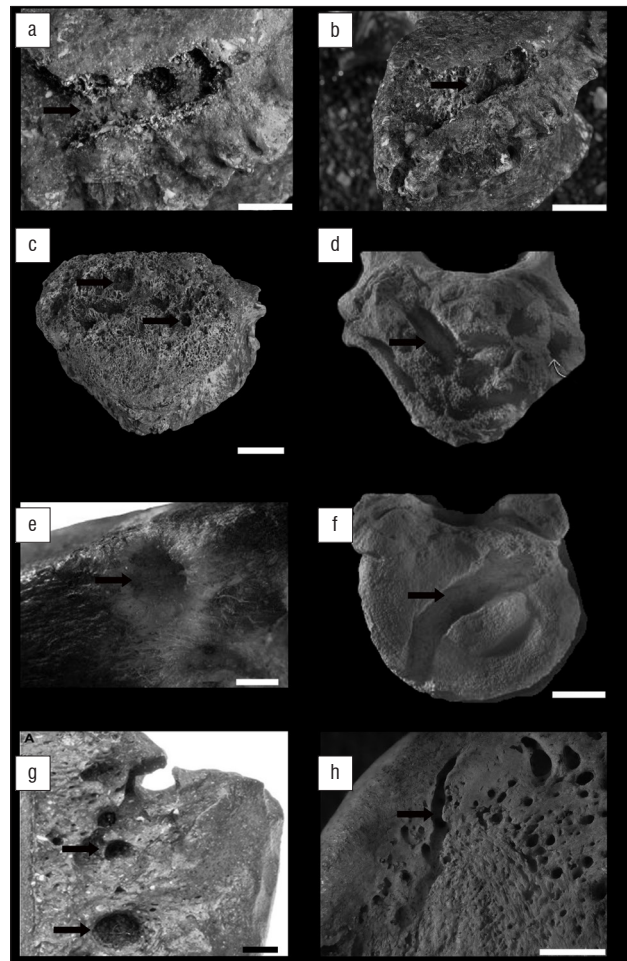
### Insect traces

A channel-like structure is present on the antero-superior margin of the L5 vertebral body (Figure 6a,b). The channel comprises a series of conjoined excavations and cavities and extends from approximately the midpoint of the antero-superior rim of the body (where the vertebra has been fractured post-mortem) until the mid-lateral antero-superior margin of the upper endplate. Externally, there is no evidence of sclerosis or reactive bone formation around the cavity margins. The channel narrows from 8 mm to 3 mm in diameter and penetrates to a maximum depth of 4 mm. Embedded in this channel are distinctive circular holes which are 3–4 mm in diameter and 3–4 mm deep (Figure 5e demonstrates this pattern in cross section). No discernible mandible marks were found in association with the insect traces. The micro-CT images demonstrate an absence of bone remodelling related to either the channel or holes.

## Discussion

### Pathology

Gross observation of surface morphology and micro-tomographic imaging of the internal cortical and trabecular morphology of the StW 431 hominin vertebrae have indicated the presence of osseous proliferation (osteophytosis) consistent with degenerative spinal joint disease. Degenerative joint disease (DJD) is one of the most common pathological ailments observed in archaeo-skeletal assemblages, and is seen in many cases as a natural internal response of the body to 'wear and tear'.<sup>25–29</sup> Skeletal involvement in DJD usually consists of the covarying processes of bone formation and bone destruction, including: (1) degeneration of articular cartilage with exposure of the bone surface, leading to progressive erosive porosity in the subchondral bone; (2) bone remodelling which produces stabilising focal nodules (osteophytes) of new bone formation at joint margins or ligament/tendon insertions (entheses); (3) subchondral cysts or lytic cavities in cartilage-depleted areas; and (4) eburation produced by direct bone-on-bone abrasion, often leaving polished wear facets on the affected areas.<sup>30–32</sup>



Scale = 10 mm

**Figure 6:** Insect traces excavated into the L5 vertebrae on StW 431 are indicated by arrows (a and b); (c) circular boring on a cercopithecus vertebra from Cooper's D; (d, f) furrows attributed to *Dermestes maculatus* from the Jurassic period<sup>34</sup>; (e) hole produced by the termite *Trinervitermes trinervoides*<sup>21</sup>; (g) holes produced by dermestids under experimental conditions<sup>39</sup>; and (h) furrow produced by the termite *T. trinervoides*<sup>21</sup>.

DJD is a chronic disease process affecting joints, particularly large weight-bearing joints and is common in older individuals, but can occur in younger individuals either through a genetic mechanism or, more commonly, because of previous joint trauma.<sup>30–32</sup> Affected individuals may express reduced mobility, reduced flexibility and chronic pain. In modern clinical practice, DJD is equally prevalent in men and women in their mid-forties to mid-fifties, although the disease has been shown to affect much younger age groups in forensic, historical and archaeological populations in individuals with physically stressful lifestyles or occupations.<sup>33</sup>

The presence of osteophytosis and other associated degenerative traits elsewhere in the lumbar and sacral region of StW 431 has been proposed by Staps<sup>18</sup> as symptomatic of spondylosis deformans in this specimen, and our results are broadly consistent with this diagnosis, although the degenerative changes observed could also be attributed to normal age-related degenerative joint changes. However, the causal mechanism behind the destructive erosion seen on L4 and L5 has yet to be unequivocally addressed from a pathological perspective and here we attribute it to post-mortem alteration by insects.

Pirrone et al.<sup>20</sup> proposed that traces in bone produced by insects can be classified into one of eight general morphological categories. Subsequently, Parkinson<sup>23</sup> synonymised grooves and striae, as well as furrows and channels, thus reducing the number of general morphological categories to only six. These categories now are: pits, holes, chambers, tubes, furrows and grooves. The insect traces identified during the course

of this study can be classified into two of these morphological categories, namely furrows and holes. Holes (Figure 6c,e,g) are considered vertical excavations in bone which display a circular morphology in plan view and a bowl-shaped morphology in cross section. Holes are primarily found embedded in the outer cortical surface or as shallow excavations which penetrate the cortical surface and terminate in the trabecular bone.<sup>20,23</sup> Furrows (Figure 6d,f,h) are horizontal excavations which present as a meandering trail across the surface of a bone. Furrows are distinguishable from chambers as they lack the characteristic ellipsoidal morphology in plan view. Furrows are constructed to variable depths, and thus either record the presence or absence of vertical walls, and in cross section either display a bowl-shaped or shallow, rounded profile (see Parkinson<sup>23(Fig.2)</sup> and Pirrone et al.<sup>20(Fig.3)</sup> for a summary of plan and cross-sectional views of these common morphologies). Thus, the primary basis for identifying the insect traces on StW 431 is morphological similarity with traces widely attributed to insects in the literature (Figure 6).

The holes identified on StW 431 have a diameter range of 3–4 mm which are within the range of holes recently reported from Cooper's D (1–8.6 mm)<sup>23</sup> (Figure 6c) and those produced by the southern African termite *T. trinervoides* under experimental conditions (1.54–3.63 mm)<sup>21</sup> (Figure 6e). However, it is necessary to compare size data to data across all morphological categories because of the transitional nature of these traces. In that the morphological categories proposed by Pirrone et al.<sup>20</sup> and Parkinson<sup>23</sup> are by no means independent of one another – it is widely accepted that they represent transitional morphotypes which relate to the orientation of the excavation relative to the bone surface.<sup>34–37</sup> For example, if an insect excavates perpendicular to the bone surface and thus penetrates vertically in the bone, the trace would transition through a number of morphologies: initially it would be a pit, transition into a hole, and culminate in a tube. Alternatively, if the excavation is orientated parallel to the bone surface, the initial excavations would potentially take the form of a chamber and culminate in a meandering furrow. The transitional nature of these morphologies is an important consideration when one compares measurement data available in the literature. Thus the holes identified on StW 431 also fall within the range of tubes reported from Swartkrans (2–5 mm)<sup>38</sup>, as well as those produced by *T. trinervoides* (3.41–4.2 mm)<sup>21</sup>. The holes on StW 431 fall outside of the range of tubes produced by *D. maculatus* (0.21–0.68 mm) and that of pits (1.5–2.5 mm) produced by dermestids<sup>39</sup> under experimental conditions (Figure 6g). Actualistic experimental results of bones exposed to *D. maculatus* suggests that dermestids rarely produce tubes or holes in bones, even after extended periods of exposure.<sup>22</sup> Lastly, the StW 431 holes also fall outside of the range of holes or tubes reported from Makapansgat which were attributed to dermestids by Kitching<sup>40</sup>.

Morphological and metrological variables are key in the identification of insect traces on bone but they have little application in identifying a specific causal agent responsible for their creation.<sup>23,35–37</sup> Traces produced by insects are morphologically consistent despite geographical and/or temporal distribution; for example, furrows as described in this study from the Plio-Pleistocene are consistent with traces recently reported from the Jurassic of China.<sup>36</sup> Shallow circular holes have been reported throughout the Mesozoic and well into the Late Cenozoic; the most commonly inferred causal agent of traces during the Mesozoic are dermestids<sup>34,41–44</sup>, but this shifts during the Cenozoic to termites being the most commonly inferred agent<sup>21,24,45–47</sup>. This temporal and geographical consistency of trace gross morphology relates to the similarity in the associated behaviour of insects whilst producing traces in bone. This unfortunate reality suggests that gross morphological categories should not be attributed to a specific agent, or should be attributed only with a high degree of caution. The trace that best illustrates this is a star-shaped pit mark.<sup>24,45</sup> Star-shaped pit marks have been widely reported from the Cenozoic of Africa and have been attributed to termites. Backwell and colleagues<sup>21</sup> sought to test this hypothesis and found that *T. trinervoides* do in fact produce star-shaped pit marks comparable to those reported in the literature.<sup>21</sup> Subsequent to this research, Parkinson<sup>22</sup> experimentally tested the impact of *D. maculatus* on bone under controlled conditions. The results of this later study suggest that dermestids also produce traces comparable to star-shaped pit marks attributed to termites. Thus inferring termites as a causal agent of star-shaped pit marks has lost a degree of

credibility because various agents can produce similar morphological traces as a result of commonality in the behaviour attributed to the trace production; this then becomes an issue of equifinality which cannot be addressed directly in the palaeorecord.<sup>22,48,49</sup>

Despite the limitations of comparing gross morphological variables across both geologically and temporally disparate traces, one solution may be to describe traces more comprehensively within an ichnotaxonomic framework.<sup>20,23,35</sup> Such a description would require establishing to what degree the traces identified on bones are distinguishable from other trace taxa described in the literature, and whether the trace is substantially different to motivate the establishment of a new ichnotaxa. For example, on a gross morphological level many traces are described as chambers, but various authors have gone one step further and formally diagnosed ichnotaxa belonging to the ichnogenus *Cubiculum*. *Cubiculum ornatus* was described by Robert and colleagues<sup>44</sup> to include traces in bone which display a chamber-like morphology but which are characterised by the additional presence of gnawing marks/grooves. Subsequently, *Cubiculum levis* was described from Argentina as a chamber which is characterised by a bowl-shaped morphology in cross section.<sup>35</sup> However, in the past 18 months *Cubiculum* has expanded to include a further two taxa: *C. inornatus*, which is similar in morphology and size to *C. ornatus* but lacks the characteristic gnawing marks/grooves<sup>36</sup>, and, most recently, *C. cooperi*, which has been described from Cooper's D in the Cradle of Humankind<sup>23</sup>. *C. cooperi* is distinguishable from all other *Cubiculum* taxa because of the absence of gnawing marks/grooves, as well as a uniquely consistent length to width ratio of 2:1.

This brief history of *Cubiculum* illustrates that at a gross morphological level, traces are broadly similar, but in fact the minor morphological variables between traces can be used as a basis for comparison and differentiation. The establishment of ichnotaxa in bone produced by insects also links morphological characteristics to the behavioural tendency of the trace makers. For example, *Cubiculum* ichnospecies are believed to represent the behaviour of producing pupation chambers in bone.<sup>23,35–37,44</sup> Interestingly, the majority of these authors who have described ichnotaxa in bone have avoided attributing a specific causal agent to the traces for various reasons.<sup>23,35–37</sup> These authors recognise that the trace is a reflection of behaviour, and that behaviour could easily be mimicked by numerous agents belonging to a diversity of insect groups. Simply put, more experimental research is required to begin to better understand and document the minor morphological variables between traces in bone produced by a substantially wider diversity of potential agents. Expanding research to address concerns of equifinality would be a fundamental step towards establishing practical criteria to enable causal agent determination/differentiation in the palaeorecord. In the case of the traces identified on StW 431, it is clear that these traces can be attributed to an insect based on gross morphological similarity to traces reported in the literature. High-resolution micro-CT provided clear evidence that the traces were produced post-mortem because there was no bone remodelling. However, because of the limited sample size and morphological and metrological similarity with traces produced by both termites and dermestids, we avoid attributing a specific agent. Lastly, the limited number of traces and lack of distinctive morphology do not warrant the diagnosis of an independent ichnotaxa, nor do the traces on StW 431 bear similarity to the existing ichnotaxa diagnosed in the region during the Plio-Pleistocene, namely *Munitusichnus pascens* and *C. cooperi*.<sup>23</sup> Lastly, drawing behavioural conclusions from a limited sample of traces which are not particularly well preserved would be futile in our opinion.

## Conclusion

Our results have demonstrated that – with the exception of the presence of osteopathological lesions in the form of osteophytic lipping, demonstrating minor degenerative joint disease – the pre-mortem bone remodelling described by previous researchers<sup>14</sup> as evidence for infectious disease is shown here to have been caused by post-mortem processes. Our results suggest that the areas described to be as a result of infection are in fact post-mortem modifications made by insects or regions exhibiting degenerative joint disease. We draw these conclusions

based upon new imaging modalities applied to the fossil specimens. This is contrast to the methods used by D'Anastasio and colleagues<sup>19</sup> which comprised observation of surface morphology using light and scanning electron microscopy. In relation to the present study, in addition to macroscopic and microscopic methods, micro-CT was used in order to achieve a much higher resolution than in previous studies with full three-dimensional capacities to model and render previously identified lesions. No previous studies have used micro-CT to evaluate the surface bone of StW 431. Until now, insect traces have not been reported on StW 431.

Macroscopic and microscopic examinations are important prerequisites to determine the difference between post-mortem taphonomic and pre-mortem pathological processes as these two processes can look extremely similar, and are difficult to distinguish. This distinction can mean the difference between an interpretation of ante-mortem pathology or post-mortem pseudopathology. The modifications observed on StW 431 cannot be considered unique, as a similar pattern of bone modification is recorded on a fossil cercopithecoid vertebra from nearby Cooper's D (Figure 6c). Skeletal material at both sites (Cooper's D and Sterkfontein) experienced similar taphonomic sequences of events. Quadrupedal and bipedal primates apparently suffered from similar joint disease conditions<sup>50</sup>, and after they died their bones appear to have been modified by an unknown insect.

This study is in agreement with previous pathological diagnoses of spinal DJD which affected StW 431, whilst shedding additional light on the complex series of post-mortem processes affecting the Sterkfontein site and its fossil assemblages. The co-occurrence of degenerative pathological processes and subsequent insect modifications of the same regions – the former being an ante-mortem in-vivo response and the latter a post-mortem or post-fossilisation modification – presents an interesting taphonomic case that may not be specific to StW 431, with a cercopithecoid vertebra from Cooper's D showing a similar taphonomic sequence of events. We suggest that it is only with a combination of traditional morphoscopic analyses of external gross morphology, coupled with non-invasive high-resolution tomographic methods (i.e. micro-CT, nano-CT or synchrotron tomography), that diagnoses can be rationalised. This comparative approach has been successfully demonstrated elsewhere in the South African fossil record, with the identification of the earliest evidence for neoplastic disease in the hominin record,<sup>51,52</sup> which would have been impossible using conventional diagnostic methods. Such caution is further supported by Mays<sup>53</sup> who suggests that, in future, secure diagnosis of infective disease processes in bone should primarily be undertaken using biomolecular means. Ancient bacterial DNA may, of course, not survive in such deep time scales, lending greater emphasis to the use of comparative non-invasive methods.<sup>51,52</sup>

## Acknowledgements

We acknowledge the assistance and help of the following people in the production of this research: Bonita de Klerk, Wilma Lawrence and Jennifer Randolph-Quinney, and the Department of Geology (Wits). We thank the Evolutionary Studies Institute Fossil Access Advisory Panel for permission to study the StW 431 skeleton and comparative fossil specimens. The research was funded by grants to L.R.B. by the National Geographic Society, the National Research Foundation of South Africa, the South African Centre of Excellence in Palaeosciences, and the Lyda Hill Foundation. Additional direct support for E.J.O. was received from the National Research Foundation of South Africa and the South African Centre of Excellence in Palaeosciences. Direct research support for P.S.R.-Q. was provided by the School of Forensic and Applied Sciences, University of Central Lancashire, UK.

## Authors' contributions

E.J.O., L.R.B. and P.S.R.-Q. wrote the original draft of the manuscript, incorporating additional information and data on Stw 431 from A.H.P., B.Z. and L.R.B., with additional palaeopathological commentary from H.B. K.J. undertook the micro-CT scanning of the hominin specimen and primary reconstruction. E.J.O. and P.S.R.-Q. undertook secondary reconstruction from orthoslice and three-dimensional volume data; all authors contributed equally to analysis and editing.

## References

1. Toussaint M, Macho GA, Tobias PV, Partridge TC, Hughes AR. The third partial skeleton of a late Pliocene hominin (Stw 431) from Sterkfontein, South Africa. *S Afr J Sci.* 2003;99:215–223.
2. Clarke RJ. Early Acheulean with *Homo habilis* at Sterkfontein. In: Tobias PV, editor. *Hominid evolution: Past, present, and future.* New York: Alan R. Liss Inc; 1985. p. 287–298.
3. Clarke RJ. On some new interpretations of Sterkfontein stratigraphy. *S Afr J Sci.* 1994;90:211–214.
4. Clarke RJ. The hominid species of Sterkfontein through time. *Am J Phys Anthropol.* 2002;suppl 34:54.
5. Wilkinson MJ. Lower-lying and possibly older fossiliferous deposits at Sterkfontein. In: Tobias PV, editor. *Hominid evolution: Past, present, and future.* New York: Alan R. Liss Inc; 1985. p. 165–170.
6. Brain CK. Cultural and taphonomic comparisons of hominids from Swartkrans and Sterkfontein. In: Delson E, editor. *Ancestors: The hard evidence.* New York: Alan R. Liss Inc; 1985. p. 72–75.
7. Stratford D, Grab S, Pickering TR. The stratigraphy and formation history of fossil- and artefact-bearing sediments in the Milner Hall, Sterkfontein Cave, South Africa: New interpretations and implications for palaeoanthropology and archaeology. *J Afr Earth Sci.* 2014;96:155–167. <http://dx.doi.org/10.1016/j.jafrearsci.2014.04.002>
8. Granger DE, Gibbon RJ, Kuman K, Clarke RJ, Bruxelles L, Caffee MW. New cosmogenic burial ages for Sterkfontein Member 2 *Australopithecus* and Member 5 Oldwan. *Nature.* 2015;522(7554):85–88. <http://dx.doi.org/10.1038/nature14268>
9. Clarke R. On the unrealistic 'revised age estimates' for Sterkfontein. *S Afr J Sci.* 2002;98(9–10):415–419.
10. Vrba ES. Early hominids in southern Africa: Updated observations on chronological and ecological background. In: Tobias PV, editor. *Hominid evolution: Past, present, and future.* New York: Alan R. Liss Inc; 1985. p. 195–200.
11. Delson E. Chronology of South African australopithecine site units. In: Grine FE, editor. *Evolutionary history of the robust australopithecines.* New York: Aldine de Gruyter; 1988. p. 317–325.
12. McKee JK, Thackeray JF, Berger LR. Faunal assemblage seriation of southern African Pliocene and Pleistocene fossil deposits. *Am J Phys Anthropol.* 1995;96(3):235–250. <http://dx.doi.org/10.1002/ajpa.1330960303>
13. Partridge T. Dating of the Sterkfontein hominids: Progress and possibilities. *Trans Roy Soc S Afr.* 2005;60(2):107–109. <http://dx.doi.org/10.1080/00359190509520486>
14. Schwarcz HP, Grün R, Tobias PV. ESR dating studies of the australopithecine site of Sterkfontein, South Africa. *J Hum Evol.* 1994;26(3):175–181. <http://dx.doi.org/10.1006/jhev.1994.1010>
15. Pickering R, Kramers JD. Re-appraisal of the stratigraphy and determination of new U-Pb dates for the Sterkfontein hominin site, South Africa. *J Hum Evol.* 2010;59(1):70–86. <http://dx.doi.org/10.1016/j.jhevol.2010.03.014>
16. McHenry HM, Berger LR. Body proportions in *Australopithecus afarensis* and *A. africanus* and the origin of the genus *Homo*. *J Hum Evol.* 1998;35:1–22. <http://dx.doi.org/10.1006/jhev.1997.0197>
17. Tobias PV. 21st Annual report of PARU and its precursors. Johannesburg: Department of Anatomy, University of the Witwatersrand; 1987.
18. Staps D. The first documented occurrence of spondylosis deformans in an early hominin. *Am J Phys Anthropol.* 2002;suppl 34:146.
19. D'Anastasio M, Zipfel B, Moggi-Cecchi J, Stanyon R, Capasso L. Possible brucellosis in an early hominin skeleton from Sterkfontein, South Africa. *PLoS One.* 2009;4(7), Art. e6439, 5 pages. <http://dx.doi.org/10.1371/journal.pone.0006439>
20. Pirrone CA, Buatois LA, Bromley RG. Ichnotaxobases for bioerosion trace fossils in bones. *J Paleontol.* 2014;88(1):195–203. <http://dx.doi.org/10.1666/11-058>
21. Backwell LR, Parkinson AH, Roberts EM, d'Errico F, Huchet JB. Criteria for identifying bone modification by termites in the fossil record. *Palaeogeogr Palaeoclimatol Palaeoecol.* 2012;337–338:72–87. <http://dx.doi.org/10.1016/j.palaeo.2012.03.032>

22. Parkinson AH. *Dermestes maculatus* and *Periplaneta americana*: Bone modification criteria and establishing their potential as climatic indicators [MSc dissertation]. Johannesburg: University of the Witwatersrand; 2013.
23. Parkinson AH. Traces of insect activity at Cooper's D fossil site (Cradle of Humankind, South Africa). *Ichnos*. 2016;23(3–4):322–339. <http://dx.doi.org/10.1080/10420940.2016.1202685>
24. Kaiser TM. Proposed fossil insect modification to fossil mammalian bone from Plio-Pleistocene hominid-bearing deposits of Laetoli (Northern Tanzania). *Ann Entomol Soc Am*. 2000;93(4):693–700. [http://dx.doi.org/10.1603/0013-8746\(2000\)093\[0693:PFIMTF\]2.0.CO;2](http://dx.doi.org/10.1603/0013-8746(2000)093[0693:PFIMTF]2.0.CO;2)
25. Agarwall SC, Grynpsas MD. Measuring and interpreting age-related loss of vertebral bone mineral density in a medieval population. *Am J Phys Anthropol*. 2009;139(2):244–252. <http://dx.doi.org/10.1002/ajpa.20977>
26. Roberts C, Cox M. Health and disease in Britain from prehistory to the present day. Stroud: Sutton Publishing; 2003.
27. Roberts CA, Manchester K. The archaeology of disease. 2nd ed. Bradford: Bradford University Press; 1996.
28. Aufderheide AC, Rodríguez-Martin C. The Cambridge encyclopedia of human paleopathology. Cambridge: Cambridge University Press; 1998.
29. Ortner DJ, Putschar WGJ. Identification of pathological conditions in human skeletal remains. Smithsonian contributions to anthropology 28. Washington DC: Smithsonian Institution Press; 1981.
30. Resnick D. Orthopedics: Diagnosis of bone and joint disorders: Volume 4. 3rd ed. Philadelphia, PA: W.B. Saunders; 1994.
31. Resnick D. Diagnosis of bone and joint disorders. 3rd ed. Philadelphia, PA: W.B. Saunders Company; 1995.
32. Resnick D, Niwayama G. Diagnosis of bone and joint disorders. 1st ed. Philadelphia, PA: Saunders; 1988.
33. Rogers J. The palaeopathology of joint disease. In: Cox M, Mays S, editors. Human osteology in archaeology and forensic science. Cambridge: Cambridge University Press; 2000. p. 163–182.
34. Britt BB, Scheetz RD, Dangerfield A. A suite of dermestid beetle traces on dinosaur bone from the Upper Jurassic Morrison Formation, Wyoming, USA. *Ichnos*. 2008;15(2):59–71. <http://dx.doi.org/10.1080/10420940701193284>
35. Pirrone CA, Buatois LA, González Riga B. A new ichnospecies of *Cubiculum* from Upper Cretaceous dinosaur bones in Western Argentina. *Ichnos*. 2014;21(4):251–260. <http://dx.doi.org/10.1080/10420940.2014.958225>
36. Xing L, Parkinson AH, Ran H, Pirrone CA, Roberts EM, Zhang J, et al. The earliest fossil evidence of bone boring by terrestrial invertebrates, examples from China and South Africa. *Hist Biol*. 2015;1–10. <http://dx.doi.org/10.1080/08912963.2015.1111884>
37. Neto VDP, Parkinson AH, Pretto FA, Soares MB, Schwanke C, Schultz CL, et al. Oldest evidence of osteophagic behavior by insects from the Triassic of Brazil. *Palaeogeogr Palaeoclimatol Palaeoecol*. 2016;453:30–41. <http://dx.doi.org/10.1016/j.palaeo.2016.03.026>
38. Newman R. The incidence of damage marks on Swartkrans fossil bones from the 1979–1986 excavations. Swartkrans: A cave's chronicle of early man: Transvaal Museum Monograph. Pretoria: Transvaal Museum; 1993. p. 217–228.
39. Holden AR, Harris JM, Timm RM. Paleoecological and taphonomic implications of insect-damaged pleistocene vertebrate remains from Rancho La Brea, southern California. *PLoS One*. 2013;8(7):e67119. <http://dx.doi.org/10.1371/journal.pone.0067119>
40. Kitching J. On some fossil arthropoda from the limeworks Makapansgat, Potgietersrus. *Palaeontol Afr*. 1980;23(6):63–68.
41. Bader KS, Hasiotis ST, Martin LD. Application of forensic science techniques to trace fossils on dinosaur bones from a quarry in the Upper Jurassic Morrison Formation, Northeastern Wyoming. *PALAIOS*. 2009;24(3):140–158. <http://dx.doi.org/10.2110/palo.2008.p08-058r>
42. Dangerfield A, Britt B, Scheetz R, Pickard M. Jurassic dinosaurs and insects: The paleoecological role of termites as carrion feeders. Paper presented at: Salt Lake City Annual Meeting; 2005 October 16–19; Salt Lake City, UT, USA.
43. Paik IS. Bone chip-filled burrows associated with bored dinosaur bone in floodplain paleosols of the Cretaceous Hasandong Formation, Korea. *Palaeogeogr Palaeoclimatol Palaeoecol*. 2000;157(3):213–225. [http://dx.doi.org/10.1016/S0031-0182\(99\)00166-2](http://dx.doi.org/10.1016/S0031-0182(99)00166-2)
44. Roberts EM, Rogers RR, Foreman BZ. Continental insect borings in dinosaur bone: Examples from the late Cretaceous of Madagascar and Utah. *J Paleo*. 2007;81(1):201–208. [http://dx.doi.org/10.1666/0022-3360\(2007\)81\[201:CIBIDB\]2.0.CO;2](http://dx.doi.org/10.1666/0022-3360(2007)81[201:CIBIDB]2.0.CO;2)
45. Fejfar O, Kaiser TM. Insect bone-modifications and palaeoecology of Oligocene mammal-bearing sites in the Doupov Mountains, Northwestern Bohemia. *Palaeontol Electron*. 2005;8(1), 11 pages. Available from: [http://palaeo-electronica.org/2005\\_1/fejfar8/fejfar8.pdf](http://palaeo-electronica.org/2005_1/fejfar8/fejfar8.pdf)
46. Hill A, Leakey M, Harris J. Damage to some fossil bones from Laetoli. Laetoli: A Pliocene site in Northern Tanzania. Oxford: Clarendon Press; 1987. p. 543–545.
47. Pomi LH, Tonni EP. Termite traces on bones from the Late Pleistocene of Argentina. *Ichnos*. 2011;18(3):166–171. <http://dx.doi.org/10.1080/10420940.2011.601374>
48. Lyman RL. The concept of equifinality in taphonomy. *J Taphonomy*. 2004;2(1):15–26.
49. Bristow J, Simms Z, Randolph-Quinney PS. Taphonomy. In: Ferguson E, editor. Forensic anthropology 2000–2010. Boca Raton, FL: CRC Press; 2011. p. 279–318. <http://dx.doi.org/10.1201/b10727-10>
50. Jurmain R. Degenerative joint disease in African great apes: An evolutionary perspective. *J Hum Evol*. 2000;39(2):185–203. <http://dx.doi.org/10.1006/jhev.2000.0413>
51. Odes EJ, Randolph-Quinney PS, Steyn M, Throckmorton Z, Smilg JS, Zipfel B, et al. Earliest hominin cancer: 1.7-million-year-old osteosarcoma from Swartkrans Cave, South Africa. *S Afr J Sci*. 2016;112(7–8), Art. #2015-0471, 5 pages. <http://dx.doi.org/10.17159/sajs.2016/20150471>
52. Randolph-Quinney PS, Williams SA, Steyn M, Meyer MR, Smilg JS, Churchill SE, et al. Osteogenic tumour in *Australopithecus sediba*: Earliest hominin evidence for neoplastic disease. *S Afr J Sci*. 2016;112(7–8), Art. #2015-0470, 7 pages. <http://dx.doi.org/10.17159/sajs.2016/20150470>
53. Mays SA. Lysis at the anterior vertebral body margin: Evidence for brucellar spondylitis? *Int J Osteoarchaeol*. 2007;17:107–118. <http://dx.doi.org/10.1002/oa.903>

